Chapter 19
Integration of Liquid-Crystalline Elastomers in MEMS/MOEMS

Antoni Sánchez-Ferrer, Núria Torras, and Jaume Esteve

19.1 Introduction

Liquid-Crystalline Elastomers (LCEs) are smart soft materials known since 1980s (Finkelmann et al. 1981, 1984; Kundler and Finkelmann 1998), but they have only recently entered to the actuator arena and Microsystems Technology. The main reason for that difficulty is related to the chemistry and compatibility of such materials with the commercial available technologies. Moreover, the huge impact and efforts for the development of inorganic materials, *i.e.*, electroactive ceramics (EACs) and shape memory alloys (SMAs), have shadowed the huge potential of LCEs. The main features of LCEs are the huge fully reversible actuation strain values up to 300 %, the range of stress values covered ranging from 100 kPa to 100 MPa, the low density of such materials around 1–2 $g \cdot cm^{-3}$, and the actuation speed from milliseconds to minutes, which are in contrast to the inorganic materials—EACs and SMAs—with very small actuation strains (up to 5 %), strong actuation stress window (from 10 MPa to 1 GPa), high density (5–8 $g \cdot cm^{-3}$), and similar actuation speed values (Huber et al. 1997). These anisotropic slightly crosslinked macromolecular compounds can incorporate different functionalities for the response to external stimuli, such temperature (Wermter and Finkelmann 2001; Thomsen et al. 2001), light (Finkelmann et al. 2001a; Li et al. 2003), or electric field (Lehmann et al. 1999; Kremer et al. 2000).

A. Sánchez-Ferrer (✉)
Department of Health Sciences & Technology (D-HEST), IFNH, ETH Zurich,
LFO Schmelzberstrasse 9, Zurich 8092, Switzerland
e-mail: antoni.sanchez@hest.ethz.ch

N. Torras • J. Esteve (✉)
Institute of Microelectronics of Barcelona, IMB-CNM (CSIC), Micro & Nano Tools Group,
Campus UAB, Bellaterra, Barcelona 08193, Spain
e-mail: nuria.torras@imb-cnm.csic.es; jaume.esteve@imb-cnm.csic.es

V.K. Thakur, M.R. Kessler (eds.), *Liquid Crystalline Polymers*,
DOI 10.1007/978-3-319-22894-5_19

Microsystems Technology is devoted to the production of new systems or components by means of microengineering techniques—sensors, actuators, and microstructured devices (Boussey 2003; Gad-el-Hak 2005)—which interact with the environment. The main advantages of microsystems over macrosystems are their reduced size and cost, as well as improved performance and versatility. Using batch processes, Microsystems Technology allows for the mass production of highly complex microstructures with feature sizes ranging from 1 μm to 100 μm (Leondes 2006; Hsu 2008).

Thus, the integration of smart soft materials, *i.e.*, LCEs into the well-known silicon-based technology goes in the direction of a new generation of hybrid MEMS and MOEMS devices which will exhibit enhanced or novel properties. Flexibility, processability and tunability are properties which LCEs bring to these new hybrid microdevices, but the main advantage of integrating LCEs is concerned to the use of external stimuli avoiding the need for any electrical connection or external controlling devices.

This Chapter aims to be an introduction to the use of LCEs in Microsystems Technology and, specifically, to the integration of such smart soft materials into MEMS/MOEMS. First, the preparation—polymerization and crosslinking—and alignment of the macroscopic sample—mechanical, magnetic, electrical, surface or viscosity alignment—, as well as the main characteristics of LCEs—actuation modes and interaction of the environment—will be presented in the Sect. 19.1. Finally, Sect. 19.2 will be devoted to the state of the art for the integration of LCEs in Microsystems Technology in the fabrication of prototypes of MEMS/MOEMS.

19.2 LCE Materials

LCEs are the combination of mesogenic molecules and crosslinked linear polymer chains (Davis 1993; Terentjev 1999; Warner and Terentjev 2007). Thus, for the synthesis of such smart materials, a mesogen, a crosslinker and a polymer backbone are needed as constituents for the final macromolecular composition (Finkelmann et al. 1981; Küpfer and Finkelmann 1991; de Jeu 2012). In the following, the chemistry used for the obtaining of LCEs for the construction of MEMS and MOEMS will be described. Moreover, an explanation for the techniques used in the orientation of the mesogenic molecules and the alignment of the polymer backbone will be presented. All LCE materials shown in this chapter, which were integrated into devices, are nematic side-chain LCEs.

The main principle for LCEs relies in the reversible order-to-disorder transition (de Gennes 1971). A common rubber material consists in a crosslinked polymer melt: a viscous liquid which mobility is reduced and fluidity suppressed due to the crosslinking of the polymer chains. When pulling a rubber band, entropy is removed and the polymer chains align along the applied mechanical field direction. After removal of this uniaxial deformation, the polymer network relaxes back to an equivalent—not equal—original polymer conformation and regaining entropy.

The relaxed disorder and the initial state before deformation is related to a random polymer coil conformation which is isotropic in nature. As soon as polymer chains start to be aligned, a global prolate conformation is achieved and the material becomes anisotropic (Noirez et al. 1988; Hardouin et al. 1994).

The key question is how this anisotropic state can be fixed and reversibly removed. The trick is the incorporation of mesogenic molecules—the so-called liquid crystals (Lehmann 1908)—which like to orient in the direction of the director in self-assembled clusters or domains. Due to the enthalpy brought by such molecules, the LCE undergoes a liquid crystal (order; enthalpy > entropy) to liquid (disorder; enthalpy < entropy) transition when the enthalpy factor is removed and entropy controls the state (Fig. 19.1a). When attached to a polymer backbone, such domains are formed but distributed randomly in all directions, as well as the polymer backbones, are also randomly aligned. This material is a polydomain of LCE, where clusters of well-ordered mesogens with stretched aligned polymer chains are distributed in all possible directions (Fig. 19.1b). The difference respect to the isotropic state is that mesogens are oriented and polymer chains adopt a prolate conformation (Schätzle and Finkelmann 1987; Wang and Warner 1987). Thus, all domains shrink in the direction of the corresponding domain local director, but since all domains do the same the average change in the dimensions is zero (Fig. 19.1b). A macroscopic change in dimensions can be only observed if a single liquid-crystalline domain is obtained (Finkelmann et al. 1984; Küpfer and Finkelmann 1994; Brand and Finkelmann 1998). In order to keep all domains oriented in the direction of one unique director, and external field should be applied and the macromolecular conformation fixed. Such monodomain of LCE is achieved by stretching of the polymer network or by orienting the mesogens if coupled to the polymer backbone, and final crosslinking. If the enthalpy brought by the mesogens is bigger than the entropy coming from the polymer network (liquid-crystalline state), the material keeps oriented and the polymer chains aligned (Fig. 19.1b). Thus, the isotropization of such liquid-crystalline domains removes the enthalpy contribution and entropy dominates the scenario (liquid state), which allows the polymer coil conformation to be reformed (Fig. 19.1a) with the corresponding contraction of the LCE sample (Fig. 19.1b). Such order-to-disorder transition is induced by means of an external field, *e.g.*, temperature (Donnio et al. 2000; Krause et al. 2007; Sánchez-Ferrer and Finkelmann 2009), light (Finkelmann et al. 2001a; Hogan et al. 2002; Sánchez-Ferrer et al. 2011a) magnetic (Kaiser et al. 2009; Winkler et al. 2010; Haberl et al. 2013) or electric fields (Chambers et al. 2006, 2009; Urayama et al. 2006).

19.2.1 LCE Components

As mentioned before, the mesogen is the component responsible for the alignment of the polymer backbone if coupling between the mesogenic molecules and the polymer backbone is present (Wang and Warner 1987). These mesogens consist in

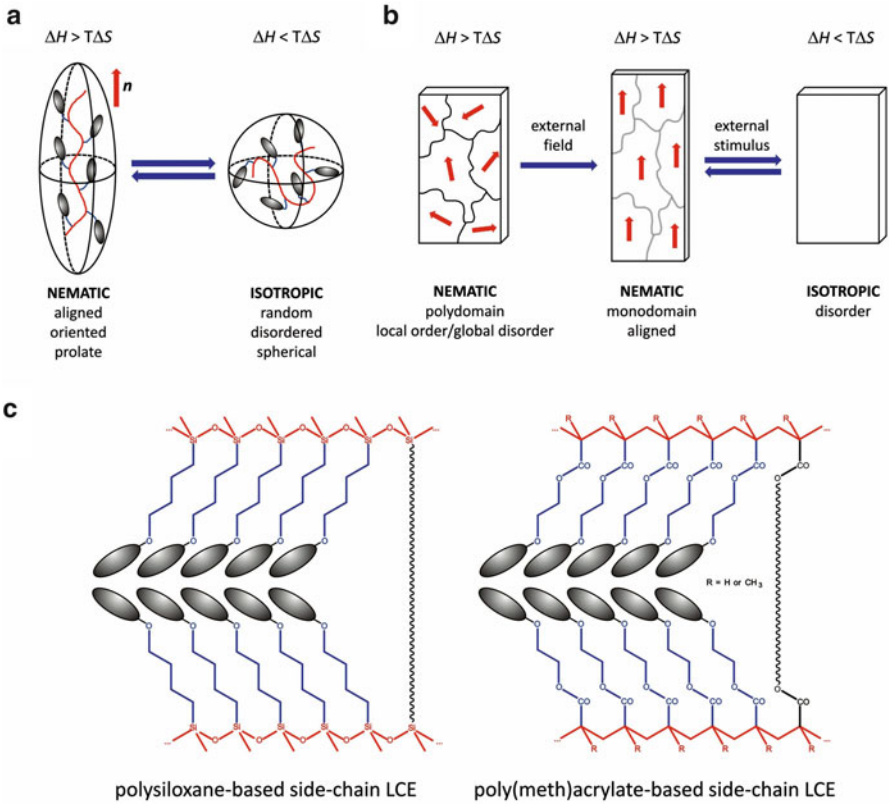

Fig. 19.1 (**a**) Nematic-to-isotropic transition in end-on side-chain LCEs; the nematic state (*left*) shows alignment of the polymer chains and the orientation of mesogens along the director, and due to the coupling between mesogens and polymer backbone a prolate conformation appears at low temperatures; the isotropic state (*right*) presents a random coil conformation of the polymer chains and disorder of the mesogens which are related to the spherical conformation at high temperatures. (**b**) Polydomain-to-monodomain transformation in LCEs; the nematic polydomain shows a random distribution (global disorder) of nematic domains (local order); the nematic polydomain has the oriented mesogens pointing in the direction of the director which is parallel to the external field and well-aligned polymer chains; the actuation principle (change in dimensions) can only be observed when the polydomain is disturbed by means of a external stimulus and reaches the isotropic state. (**c**) Chemical structure for both end-on polysiloxane-based and poly(meth)acrylate-base side-chain LCE, where the polymer backbone (*red*), the spacer (*blue*), the rod-like core (*grey*) and the crosslinker (*black*) are depicted

a two or more aromatic rod-like molecule (crystalline component) with at least one reactive flexible aliphatic spacer (liquid component). Such molecules are directly attached to the polymer backbone as side groups (side-chain LCEs) or forming part of the polymer backbone (main-chain LCEs). The aromatic core allows for the self-assembly of the mesogenic molecules, while the flexible spacer brings mobility and affects the polymer backbone. The increasing number of aromatic rings increases

the mesophase stability, and rises the isotropization temperature due to a better interaction between the cores. The spacer should neither be too short—allowing some freedom to the polymer backbone—nor too long—no coupling between the mesogens and the polymer backbone (Wermter and Finkelmann 2001; Tajbakhsh and Terentjev 2001). Usually, an odd number of atoms in the spacer (even number of carbons) lead towards a polymer chain prolate conformation (Fig. 19.1a). Finally, mesogens might show just orientational order (nematic phase) or also positional order (smectic phase)—which is related to a more energetically rich mesogen (Sánchez-Ferrer and Finkelmann 2009). A nematic mesogen has a nematic-to-isotropic transition temperature T_{ni}, while a smectic mesogen has a smectic-to-isotropic transition temperature T_{si}, even that other order-to-order transitions can be observed.

The polymer backbone can be a polymer melt (amorphous liquid polymer; low glass transition temperature T_g), *i.e.*, polysiloxanes, or a polymer glass (amorphous glassy polymer; high glass transition temperature T_g), *i.e.*, polyacrylates and polymethacrylates. For the first ones, each hydrogenmethylsiloxane repeating unit reacts with a vinyl double bond from the mesogen or crosslinker via hydrosilylation reaction (Küpfer and Finkelmann 1991, 1994). The resulting material is a low T_g mesogenic network or side-chain LCE (Fig. 19.1c). Polyacrylates and polymethacrylates liquid-crystalline networks (LCNs) are formed when the reactive mesogen polymerizes via radical polymerization with a (photo)-initiator. The obtained material is a high T_g mesogenic network which strictly speaking is not an elastomer at room temperature, but can be found as LCE in the literature and considered as such at temperatures above the T_g.

Finally, the crosslinker is the responsible to keep the polymer chains together and, more important, to fix the alignment when a monodomain is obtained. This molecule is a bifunctional—only for side-chain LCEs (Küpfer and Finkelmann 1991, 1994)—or a multifunctional molecule—for both side-chain and main-chain LCEs (Donnio et al. 2000; Sánchez-Ferrer and Finkelmann 2009). Crosslinkers can be either flexible (isotropic) or rigid (liquid-crystalline), and reduce the mobility of the polymer backbone, therefore increasing the materials' T_g. Moreover, it should be mentioned that a flexible crosslinker acts as an impurity, destabilizes the nematic phase, and reduces the T_{ni}; a rigid crosslinker stabilizes the mesophase and raises the T_{ni}. Usually flexible crosslinkers are used for polysiloxane-based LCEs, and rigid mesogenic crosslinkers are mainly used in polyacrylate and polymethacrylate-based LCNs. Special attention should be given to photo-crosslinkers, which can be used in both chemistries and are mainly flexible (Komp et al. 2005; Beyer et al. 2007; Sánchez-Ferrer et al. 2009). The amount of crosslinker will be a very important factor for the mechanical properties and actuation behavior of the LCE systems. Lightly crosslinked LCEs will show huge deformations but small retractive forces; highly crosslinked LCEs show small changes in dimensions but huge actuation forces. Thus, the right amount of crosslinker, as well as the mesophase which determines the working range of temperatures (T_{ni}–T_g), is the key point for the obtaining of tunable actuators and sensors.

19.2.2 Mesogen Orientation and Polymer Alignment

Monodomains of LCEs based in polysiloxane polycondensation chemistry has been obtained by two main processes. The first process is the so-called two-steps crosslinking process (Brand and Finkelmann 1998), where in a first step mesogens are attached to the polymer backbone and the polymer chains are partially crosslinked. The obtained swollen network or isotropic gel is mechanically deformed, *i.e.*, uniaxially stretched (Küpfer and Finkelmann 1994) or biaxially compressed (Torras et al. 2013). The second step consists in the completion of the crosslinking in order to fix the deformation while removing the solvent by evaporation. The second process relates to the use of magnetic/electrostatic fields. A liquid-crystalline polymer which contains a photo-crosslinker is synthesized. This polymer is annealed right below the isotropization temperature and the mesogens oriented under a magnetic field (Komp et al. 2005; Sánchez-Ferrer et al. 2009). Due to the coupling between the mesogens and the polymer backbone, the polymer chains' alignment is achieved. Afterwards, the sample is crosslinked by means of UV light. Samples of thickness ranging from hundreds to thousands of microns can be produced by the two-steps crosslinking process, while samples of tens of microns can be only produces by photo-crosslinking. Moreover, the first processing allows for huge deformations/actuations—up to 70 %—because the polymer chains are aligned by means of the mechanical deformation, and this alignment orients the mesogens due to the coupling between the two components. These materials can only be processed after the synthesis and integrated in a *Top-Down* approach. The UV-crosslinking process relies on the orientation of the mesogens which should stretch the polymer chains, but should overcome viscosity and polymer conformational issues. Thus, small deformations/actuations—up to 20 %—can be achieved. This technique allows also for the integration into devices before the final material is obtained in a *Bottom-Up* approach by the use of photo-masks.

Monodomains of LCEs based in poly(meth)acrylate polyaddition chemistry can be produced by a single process. Mesogen, crosslinker and (photo)-initiator are put together (Thomsen et al. 2001; Haseloh and Zentel 2009; Ohm et al. 2009). The mixture reacts forming the polymer backbone and the simultaneous statistical crosslinking of the polymer chains as they grow. This process is done under orientational techniques such surface effects or capillarity forces. Both techniques allow for the orientation of the rod-like molecules, but the order can only be kept for few microns gap/thickness, which is enough to see some bending/actuation in the samples. Thus, due to the rigidity of the polymer backbone (high T_g), the small thickness of the obtained samples and the high working temperatures, applications are reduced to very small devices. A good advantage is that the material can be integrated in one single process following a *Bottom-Up* approach as used in display technology applications. Hundreds microns thickness samples can be obtained by using a nematic solvent and magnetic fields, where the solvent helps to reduce the viscosity of the mixture, the clearing temperature during the network formation,

and enhances the orientation of the mesogens (Urayama et al. 2007; Urayama 2010). Formally speaking, the material is a gel which can be deswollen and a LCN can be obtained, but the material has to be integrated to the device afterwards in a *Top-Down* approach.

19.2.3 Actuation Principles

As mentioned in the previous chapter, the nematic-to-isotropic transition has to take place in order to induce disorder in the mesophase (between the mesogens), and the corresponding misalignment of the polymer chains which adopt the entropically favorable coil conformation (Fig. 19.1a). This isotropization process needs for a trigger or external stimulus which brings energy to the system by rising the temperature or by introducing impurities to the system. For the first case, heat or heat-related stimuli are used; *e.g.*, direct heat from the surroundings which is transferred through the sample (Wermter and Finkelmann 2001), or due to Joule effect when some electrical current is applied through a dissipative medium (Chambers et al. 2009), or non-selective absorption of a photon in the visible or infrared region which locally releases heat after the corresponding electron relaxes in a non-radiative way (Ji et al. 2012; Haberl et al. 2014). For the second case, the change in shape of a molecule which disturbs the liquid-crystalline phase is required. Thus, the most common external stimulus used here is light which induces the photo-isomerization of photo-active molecules (Sánchez-Ferrer 2011; Sánchez-Ferrer and Finkelmann 2013). Such isomers obtained after irradiation shift the isotropization temperature of the liquid-crystalline phase by changing the chemical composition, but not raising the temperature. Moreover, the architecture of such molecules can be modified in a way that they connect different polymer chains which are forced to come together after irradiation. Of course, other stimuli can be considered, but up to now only those described above have been implemented in MEMS/MOEMS due to their easy applicability and affordability.

The sort of actuation which can be produced by nematic side-chain LCEs strongly depends on the chemistry, as well as the orientation/alignment used for the obtaining of monodomains. Thus, LCEs can easily produce contraction and/or expansion no matter the thickness, dimensions or shapes of the actuator. These prolate samples which are uniaxially stretched undergo contraction along the direction of the deformation when disordered, while expand in the other two directions perpendicular to the imposed deformation (Küpfer and Finkelmann 1994). For those prolate samples biaxially stretched, expansion along the imposed deformation occurs accompanied by a contraction in the other two perpendicular directions (Torras et al. 2013). LCEs which are devoted for light-induced actuation—photo-isomerization—, suffer of huge absorption of photons already in the first microns. This problem related to the penetration depth of selective photons is the main responsible for the natural bending of such LCEs. Nevertheless, a solution is to use a huge amount of photons together with an optimal amount of photo-active

molecules with high quantum yield and faster response. Then, the first layers will absorb the selected photon becoming inactive upon reaching the photo-stationary equilibrium—open window—, and allowing the photo-isomerization of the next layers—close windows (Knežević and Warner 2013).

Nevertheless, in order to achieve a homogeneous contraction/expansion of the LCEs, the applied external stimulus should be applied equally in all directions, otherwise bending or more complicated modes will be observed. This issue can be avoided by preparing very thin samples and by using local heat, *i.e.*, absorption of non-selective light by nanoparticles (Ji et al. 2012; Haberl et al. 2013), hyperthermia produced by alternating magnetic fields (Kaiser et al. 2009; Winkler et al. 2010), Joule effect by applying electrical current through in-sample conductors (Chambers et al. 2009; Sánchez-Ferrer et al. 2009), or by means of huge electrostatic fields applied to a sandwiched thin film (Urayama et al. 2006, 2007).

When bending modes are required without any photo-active molecule present in the LCE sample, the construction of a bilayer system is needed. Another material with different thermal expansion/contraction coefficient or elastic modulus will be attached to the LCE actuator. Thus, the surface of the bulk LCE directly attached to the passive material will not actuate due to mechanical restrictions, while the rest of the LCE material far from the interface will deform. Such deformation of LCE actuator will happen showing a gradient from zero at the interface to the maximum value in the surface far away from the other material. Actually, this actuation principle is always occurring when a LCE object is chemically attached to solid-like surface, *e.g.*, silicon, metal oxide, glass.

Finally, other aspects to be considered are the actuation force and the time response of LCE devices. While actuation forces are directly related to the crosslinking density—highly crosslinked LCEs show huge actuation forces, and low crosslinked LCEs have huge deformations—, the time response strongly depends on the interaction between the external stimulus and the LCE material. LCEs are polymer-like materials and the thermal conductivity is close to that of insulators. Thus, to achieve homogeneous isotropization temperatures along the sample cross section, the material needs minutes to reach the equilibrium temperature. The use of light is directly connected to the nature of the photo-active molecule incorporated into the network, and to the kinetics related to the photo-isomerization process which at room temperature is in the range of minutes too. A very good approach is the incorporation of heat-release systems which have lowered the response time to values in the range of milliseconds, *e.g.*, nanoparticles, micro-heaters.

19.3 Integration of LCEs into Microsystems Technologies

In the field of engineering, silicon-based technologies are the most commonly used for the fabrication of microsystems (Maluf and Williams 2003). These well-known techniques are very robust and well-controlled, and allow a batch processing

large-scale fabrication of devices combining a large number of varied physico-chemical processes, *e.g.*, deposition and growth of layers, etching techniques, shaping and patterning of these deposited layers (Merlos et al. 1993; Judy 2001). Furthermore, these processes enable the use of several types of materials ranging from silicon and its derivatives to polymers, metals and oxides. In this manner, it is possible to fabricate various types of devices like simple resistors, micro-heaters and transistors for circuitry (Snyder et al. 2003), accelerometers for ITC technologies and automotive field (Plaza et al. 2002), radiation detectors (Lutz 1999), bio-devices (Grayson et al. 2004) and solar cells for energy harvesting (Cook-Chennault et al. 2008), among others.

Nowadays, new materials and techniques have been introduced to the standard fabrication processes in microelectronics in order to obtain more complex systems and hybrid devices with new and interesting properties (Yang and Wang 2004; Dai et al. 2007; Liu 2007). Among conventional materials, polymers are the best example. They are flexible, soft, inert, ease to be processed and cheap, and have a large number of very interesting tunable properties which can be adapted to a specific needs and situations. Soft lithography techniques (Lorenz et al. 1997; Xia and Whitesides 1998), flexible substrates for printed electronics (Berggren et al. 2007), packaging of lab-on-a-chip devices and microfluidic systems (Dittrich and Manz 2006; Haeberle and Zengerle 2007) are some examples of the growing use of polymers in microsystems technology. However, the integration of polymers into MEMS/MOEMS devices as active elements is still a challenge since most of the silicon processing techniques require high working temperatures—hundreds of degrees—, and the use of aggressive chemical agents such as potassium hydroxide (KOH), tetramethylammonium hydroxide (TMAH) and hydrofluoric acid (HF) which can damage polymeric materials.

As previously mentioned, it is well-known that nematic LCEs can cause macroscopically stimuli-responsive shape changes during the nematic-to-isotropic phase transition, resulting from the microscopic disorder and misalignment of their components. Due to the reversibility of such nematic systems, when the external stimulus is removed, LCEs can produce actuation.

Back in the 1970s, when P.G. de Gennes proposed for the first time the possibility of using LCEs as artificial muscles (de Gennes 1971, 1975, 1993), monodomains of LCE materials have been widely studied leading to a large number of scientific publications and studies, and they have been proposed for the fabrication of active devices (de Gennes 1997; Woltman et al. 2007; Ohm et al. 2010) due to the big change in shape and length when disorder is induced by and external stimulus. However, LCE materials should be aligned (monodomain) and the mesogens properly oriented in a defined direction. The orientation of mesogens and alignment of the polymer backbones in LCEs before or after the final fixation of the polymer chains in the macromolecule requires the use of external fields which will simultaneously shape the material. This requisite strongly affects the use of the LCEs as actuators, and limits the integration into MEMS/MOEMS devices for the fabrication of real-world applications.

In the following, we present examples from the literature in which LCE materials have been proposed as actuators and sensors. These examples have been grouped in two different groups as function of the strategy followed for the integration of the material into the system to give rise to the final device. That is before or after the crosslinking process is finished.

In the first part, we will review the applications based on the integration of oriented LCE films which has been previously synthesized—mesogens oriented and polymer chains aligned and fixed by full crosslinking of the material. In the second part, other types of actuators and sensors based on alternative procedures will be presented where such choice allows for the in-situ orientation and alignment prior total fixation of the LCE while integrating the material into the device at the same time.

19.3.1 Integration of Ex Situ *Fully-Crosslinked LCEs*

The devices herein described are based on the integration of nematic films which have been previously aligned and cured. Thus, the shape and dimensions, and the corresponding change in those two parameters are limited to the degree of deformation imposed to the film during the synthesis. Usually, LCE films are obtained by 1D alignment—stretching of the sample in one direction before the final crosslinking—that produces a shortening in the direction of the deformation when the liquid-crystalline order is removed.

The first four examples presented are based on silicone polymeric matrices with T_g below 0 °C, and T_{ni} ranging from 55 °C to 90 °C, which have been grouped in two as function of their actuation mechanism. On the one hand, a microgripper and a microvalve which actuation is controlled by direct heating (*i.e.*, Joule effect), and on the other hand, a heliotropic system and a tactile device both based on local heating through light irradiation, thanks to the use of LCE nanocomposites. The last three examples discussed are based on acrylate chemistry with higher T_g (above room temperature) and T_{ni} (up to 170 °C) than the silicone-based LCE samples. Due to these high T_g values only thin films can be considered which can produce bending motion under illumination when doped with photoactive molecules or stretching when raising temperature locally.

As previously reported in Sect. 19.2, there is a preferred way for the fabrication of oriented films. The synthetic concept is essentially based on the partial crosslinking of the material in order to form a weakly crosslinked film in which a uniform uniaxial deformation of the sample is applied allowing the alignment of the polymer chains along the direction of the imposed stretching. After a successful deformation of the sample, the film is further crosslinked (curing process) in order to fix the alignment and create fully functional monodomain. At this moment, the LCE film is ready to be integrated on the device, so they can be carefully cut in a desired shape and then fixed into the structure, ensuring a correct adhesion and therefore a desired actuation.

This concept was firstly reported by Bründel et al. (2004) who demonstrated for the first time the possibility to integrate LCE materials into MEMS/MOEMS systems, and the compatibility of such materials with some of the manufacturing processing techniques in microelectronics. Following this principle, Sánchez-Ferrer et al. (2009) introduced the first LCE-driven silicon microsystem: a microgripper based on the thermal actuation of a monodomain LCE film, showing temperature-controlled motions. Figure 19.2a shows a schematic representation of the device with the main parts, as well as pictures of the final device and its actuation principle. For the obtaining of the nematic polysiloxane-based LCE material, a side-chain nematic liquid-crystalline polymer (LCP) containing photo-reactive moieties, which allow the crosslinking of the polymer chains, was synthesized and oriented using a magnetic field of 11 T or an electrostatic field of 300 $kV \cdot m^{-1}$. The photo-crosslinking of the LCP chains using UV light resulted in a monodomain of LCE sample of about 16 mm × 4 mm × 0.030 mm, with a T_{ni} ranging from 59 °C to 67 °C as function of the photo-crosslinkable benzophenone units content (10 mol% and 5 mol%, respectively). The microsystem was fabricated combining standard photo-lithographic and etching processes, typical from batch MEMS/MOEMS manufacturing and the elastomer was finally mounted onto the microgripper arms and fixed using oxygen plasma to assure good adhesion between the two surfaces. The design and the distance between both microgripper arms were fixed in agreement with the LCE samples characteristics to ensure its correct operation for reaching the maximum strain values. A controlled heating induced by the voltage applied on the extremes of the gold wires wounded around the LCE film triggered the LCE phase transition, leading to movement of the microgripper arms and changing their positioning due to the mechanical stresses. Small changes in the LCE film produced actuation stress of up to 60 kPa and deformation strain of up to 150 % when applying electric voltage values ranging between 1.5 V and 3.5 V, which strongly vary the actuation times of the device from 1.6 min to 46.1 min, and thus the hysteresis factor, which increases significantly while reducing the times of actuation. Using this approach, it has been demonstrated that large and robust contractions of LCE material can be integrated on a microsystem and used to induce a mechanical response on it, envisioning the possibility for the use of this actuation principle into other technological applications.

Later on, Sánchez-Ferrer et al. (2011b) reported another example when integrating a side-chain nematic polysiloxane-based monodomain of a LCE into MEMS/MOEMS by developing a flow regulating microvalve for microfluidics. The actuation principle was basically the same than the previous example, but advantage was taken from the expansion of the material in the other two directions perpendicular to the alignment and bending of the LCE in the direction of the liquid flow which allowed the closing of the microvalve upon the nematic-to-isotropic phase transitions of the material. Thus, opening and sealing of the microfluidic channel was achieved when going back and forward from the isotropic to the nematic state. A schematic view of the structure designed, as well as a sequence of images of the microvalve performance and the corresponding actuation plots are depicted in Fig. 19.2b. The volumetric flow of the medium is guided underneath the actuator

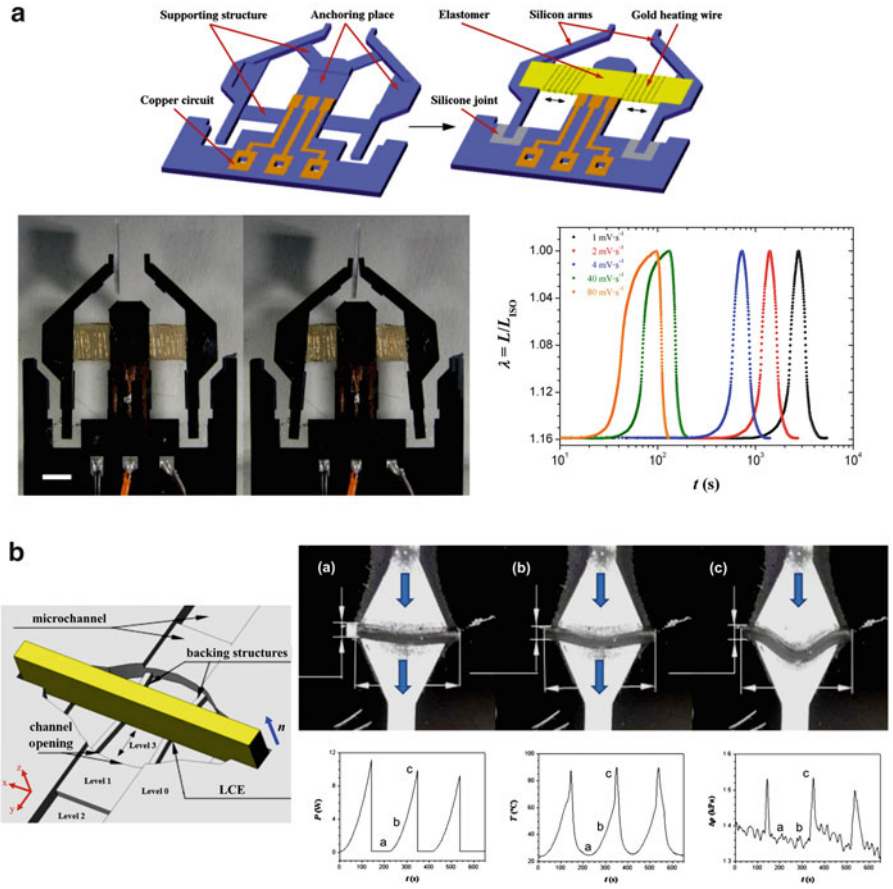

Fig. 19.2 Integration of polysiloxane-based side-chain nematic LCE in Microsystems. (**a**) Preparation of the silicon frame together with the copper electrical circuit and integration of the LCEs with the gold heating wires and the silicone joints before removal of the silicon supporting structures; two pictures showing the mechanical actuation of the LCE microgripper before and after contraction of both LCE films when heating disorder is produced; contraction of the LCE films as function of time at different voltage rates; and (**b**) integration of the LCE into the microchamber before sealing and the obtaining of the microvalve; sequence of pictures showing the positioning of the LCE film in (a) the nematic phase when the microvalve is fully open, (b) when approaching the isotropic temperature and the microvalve starts closing, and (c) when fully isotropic and the microvalve is closed (*Note*: the *blue arrows* show the liquid flow direction); electrical power, temperature of the microchamber and differential pressure between the two openings as function of time when closing the microvalve—the letters correspond to the pictures described before

(Level 3). A small supporting structure on the chip, which is on the same level as the bearing surfaces for the two ends of the actuator (Level 2) prevents buckling in the normal direction. Thus, the deformation of the valve in the main direction cannot be avoided and is compensated by an elevated channel ground (Level 1). Two identical

micromachined chips were assembled together face to face to form the microfluidic system including a 0.66 mm × 3.8 mm × 0.30 mm LCE actuator in between as a moving valve. One part of the assembled chip contains a copper circuit on its back side for heating, while the backside of the microchip has the electric contacts and a thermoresistor to measure the temperature as function of the applied electric power. For the fabrication of the microvalve, a nematic monodomain of a side-chain LCE was synthesized following the two-step crosslinking process outlined by Finkelmann et al. (2001b).

As shown in the sequence of images in Fig. 19.2b, the LCE microvalve sealed the structure upon heating and filling the room in the directions perpendicular to the director and to the liquid flow up to the wall. When the LCE film reached the wall and tension grew, an abrupt buckling of the actuator occurred in the middle of the LCE film closing the microchannel in the direction of the flow. This middle part of the actuator moved to the microchamber blocking the fluid flow and creating an extra pressure due to the self-clamping at the two ends. The shrinkage of the actuator in the parallel direction to the director aided its movement in the microchamber as a result from a reduction of the friction forces between the actuator and the microstructure. In that case, the maximum heating power applied was 11 W at a volumetric flow rate of 271 $\mu L \cdot s^{-1}$ using water; values which can be improved by reducing the heating power dissipation by changing the fluid type if not swelling of the LCE material is present (bad solvent).

It has been demonstrated that LCE are robust materials which can be tuned to adapt their responsiveness to certain external stimuli. Thus, by the incorporation of nano-objects such as carbon nanotubes (CNTs), ferro/ferrimagnetic nanoparticles, photo-sensitive particles or molecules, etc. within the polymeric matrix, it is possible to create custom-made LCE nanocomposites with different functionalities (Ji et al. 2012). Among others, CNTs are of special interest due to their morphology intrinsic characteristics and photon absorption (Saito et al. 1998; Tombler et al. 2000). When embedded into a polymer matrix, CNTs act as local heaters, as they efficiently absorb light photons along all the visible-infrared (Vis-IR) spectrum converting electromagnetic energy into thermal energy (Ajayan et al. 2002; Cantournet et al. 2007). Thus, thermal energy can be directly and wireless delivered all over the thickness of the LCE film resulting in a faster material response compared to direct external heating. In addition, neither significant effect on the LC order nor in the internal structure of the elastomer has been observed for concentrations below 1 wt% (Marshall et al. 2012), resulting in no differences in the mechanical response compared to the sample without CNTs. All of that leads to the photo-thermomechanical actuation of LCE which is a more suitable mechanism for many engineering applications, since faster actuation responses can be obtained with remote control on the actuation, and the complexity of the setups can be reduced. However, the use of this type of LCE nanocomposites involves a more elaborated process for the preparation of the samples, which entails the addition of other chemical compounds such as surfactants to avoid the formation of CNTs aggregates, and to ensure a homogenous dispersion of the elements throughout the whole sample (Ji et al. 2010, 2011).

Pursuing this actuation mechanism, two different actuators have been reported, both of them using LCE nanocomposites, which demonstrated the suitability of this type of actuation. Li et al. (2012) reported a novel mechanism based on the direct actuation of the nematic material by means of sunlight. In this way, the authors were capable to emulate the heliotropism observed in nature. The material used for this study consisted in LCE-CNT nanocomposite reinforced with a polyurethane fiber-network in order to increase the mechanical stability of the system, but causing a significant increase of the power requirements.

Torras et al. (2014a) proposed the first complete device based on photo-mechanical actuation of an array of LCE-CNTs capable to emulate Braille characters. Thanks to the combination of nematic LCE-CNT films together with a well-designed optical system, an array of hundred actuators with pushing forces was obtained. The actuation time was lower than 10 s with forces up to 45 mN far enough for lifting the pin when shining the material with a white light source.

Inspired in the heliotropism present in nature, Li et al. (2012) developed an artificial system directly driven by the sunlight. The main driving force is the photo-thermal actuation of a nematic LCE nanocomposite. The LCE-CNT actuator was fabricated using a two-steps crosslinking process in which single-walled CNTs (SWCNTs) were incorporated into a side-chain LCE matrix reinforced by a polyurethane continuous fiber-network in order to improve the mechanical performance at rupture and oriented by means of uniaxial stretching (Li et al. 2011; Jiang et al. 2013). The resulting fiber-network/SWCNT/LCE material has a T_{ni} around 68 °C. A scheme of the device and the working principle of the heliotropic system are shown in Fig. 19.3a, where the different components can be distinguished. Similar to a stool, the device consists of a platform which contains a solar cell panel supported by some actuators. Thanks to the special design the structure consists of light concentrators, heat collectors and elastic supports. The pieces of actuator facing the incoming sunlight receive enough electromagnetic energy which is converted into local heat inducing disorder in the liquid-crystalline material. Thus, this local disorder induces the macroscopic contraction of the material, driving and tilting the platform towards the sunlight (Fig. 19.3a). On the other hand, the other pieces of actuator not exposed to the sunlight remain in the relaxed state. The mechanism was tested in both in-field via direct actuation by sunlight, and in laboratory conditions using a white light source at 100 $mW \cdot cm^{-2}$ of power density. Both experiments showed an increase in the output photo-current of the solar cells, and these results proved the use of this artificial heliotropic mechanism for future energy harvesting applications.

Another interesting example where LCE nanocomposites were used was presented by Torras et al. (2014a) for the development of a tactile device. Such device consists on nematic LCE-CNT-based films integrated into an array of 10×10 photo-actuators able to represent Braille characters and simplified graphical information. These films were individually assembled in U-shape-like configuration forming single Braille elements, and later integrated in the optical device which consists in arrays of white LEDs with mirrors and lenses in order to focus all photons on the surface of the LCE-CNT film under illumination. In this way, when

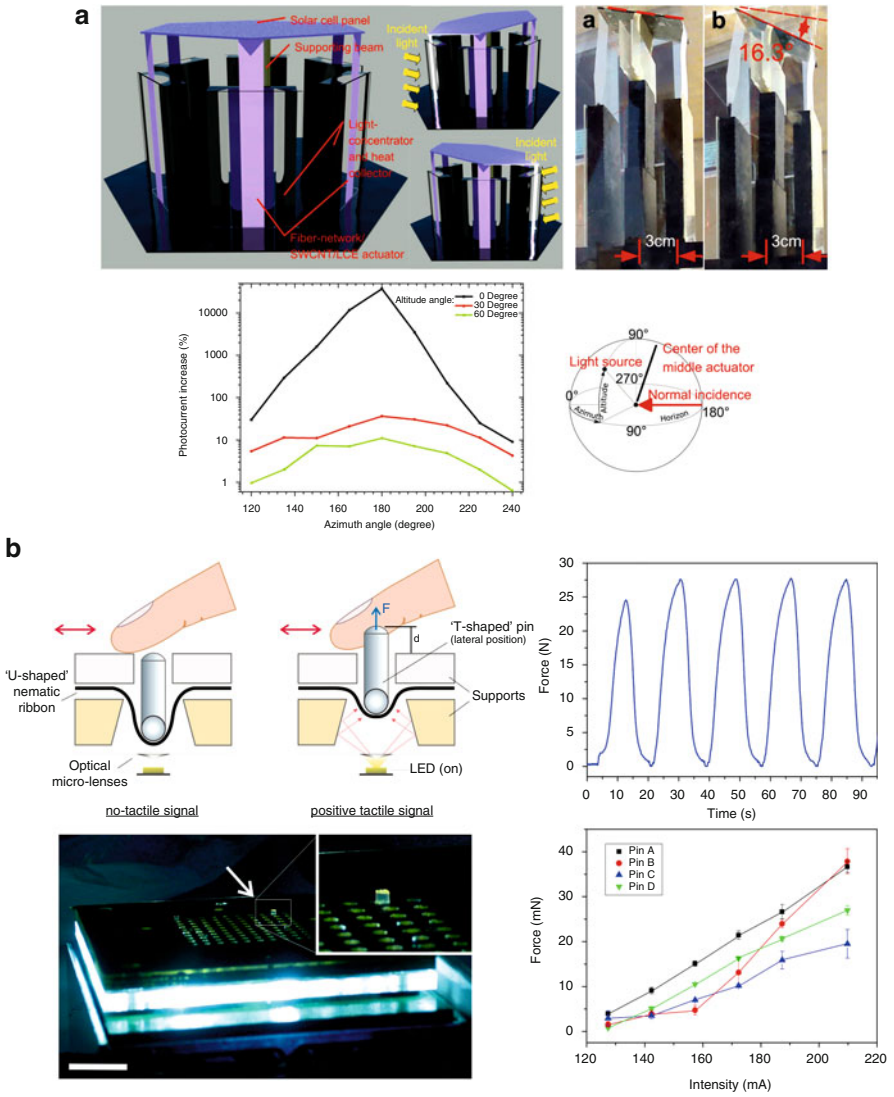

Fig. 19.3 Hybrid systems based on the integration of LCE nanocomposites. (**a**) Orientation principle (heliotropism) for the fiber-network/SWCNT/LCE device showing how the solar cell panel on the top orients when sun illuminates the contracting strip facing the sunlight; two pictures before and during illumination of the device where a small change in LCE-CNT actuators length induces a tilt angle in the solar cell panel; Photo-current intensity increase as function of the azimuthal angle at different altitude with respect to the equator showing a maximum intensity at 180° when a maximum of sunlight flux is achieved; and (**b**) schematic and actuation principle for the MOMS tactile device based on an array of LCE-CNT actuators able to represent Braille characters (scale bar = 10 mm); Force as function of time for the tactile device showing its reproducibility in several on/off cycles; picture of the tactile device with a pin lifted upon illumination; force as function of the electrical intensity applied to different LEDs lifting the corresponding pin

shining on the LCE-CNT, light is absorbed by the CNT which raise the local temperature and contract the U-shape part of the film. The light-induced stress gradient generated by the nematic LCE-CNT upon illumination produces a vertical displacement of corresponding movable pin, which transmits the tactile signal to the user's fingertip. A detailed scheme of an assembled actuator with all components is depicted in Fig. 19.3b. For the fabrication of such one hundred pin device, 1.2 mm wide and 0.3–0.4 mm thickness side-chain LCE-CNT ribbons containing 0.1 wt% of multi-walled carbon nanotubes (MWCNTs) were synthesized and mechanically stretched following the standard two-steps crosslinking process (Küpfer and Finkelmann 1991). The working temperature range for this composite goes from of $T_g \approx 10$–15 °C to $T_{ni} \approx 85$–90 °C. The LCE-CNT ribbons were assembled in a U-shaped configuration to warrant no-tactile signal when the light source is switched off (rest position), and at the same time, a positive tactile signal under illumination. T-shaped rounded pins of 0.8 mm in diameter were placed inverted on top of the LCE-CNT ribbons to maximize the contact area and thus the force transmission. Additional elements such as Fresnel micro-lenses together with refractive supports were specially designed and incorporated into the device to improve the optical path efficiency and to optimize the working parameters of the device. Lower actuation times (between 3.5 s and 8 s as function of the light intensity) and pins' displacements of $0.8\,\text{mm} \pm 0.2$ mm were obtained with measured forces of up to 40 mN without material degradation; values which guarantee a correct tactile perception and fit the Braille standards, proving not only the viability of the device but also the potential applications of this type of actuator. Hardware implementation and a communication software interface were also developed adapting the standard Bluetooth and UBS protocols to provide end users with a complete and portable solution.

The four examples described so far are based on polysiloxane matrices which allow the possibility to obtain deformations of the whole sample (contraction and expansion movements) and relatively high actuation forces. This chemistry has also the advantage of having the nematic phase above the glassy state ($T_g < 0$ °C) and below the isotropic state ($T_{ni} < 90$ °C), which lower the power requirements in order to reach actuation. On the contrary, the following three examples to be discussed are based on acrylate chemistry which presents higher glass transition and clearing temperatures. This up-shifted temperature working window together with an increased rigidity of the polymer backbones results in a drastically reduction on the mobility of such films. For this reason, the thickness of liquid-crystalline polyacrylate-based films should be in the range of few microns in order to produce any movement, *i.e.*, bending, since the actuation mechanism mainly occurs on the surface of the sample. The first example, outlined by Yamada et al. (2008), takes advantage of the combination of both UV and visible light to induce the rotation of a plastic motor consisting of a set of two pulleys and an azobenzene-containing LCE film as a belt. Using a similar procedure, Chen et al. (2010) reported a light-driven micropump based on the bending and unbending motion of a LC membrane which produces pressure gradients, and thus the movement of the fluid. In the last

example, Petsch et al. (2014) posed LC films with embedded deformable thermoresistors as a way to faster deliver heat along the sample.

As previously introduced, Yamada et al. (2008) presented the light-induced rotation of a motor based on azobenzene-containing side-chain LCE films at room temperature. The main actuation principle relies on the *trans*-to-*cis* disorder-induced photo-isomerization upon UV-irradiation, and the order-induced *cis*-to-*trans* photo-back-isomerization with visible light. By the simultaneous irradiation using both UV and visible light in opposite sides of a LCE ring, the combination of intermittent contraction and expansion movements results in a rolling motion of the film, which drives the two pulleys forming the motor. A scheme showing the working principle of the device is depicted in Fig. 19.4a, where the main elements forming the device can be identified. An example of the photo-induced motion of the motor in a counterclockwise direction is depicted in the sequence of images below. In order to reinforce the LCE film and thus improve its mechanical properties, a 50 μm thick flexible polyethylene (PE) sheet was attached on the photo-crosslinked azobenzene-containing LCE ribbon by thermal bonding creating a 68 μm thick laminated film, which was used to form the motor belt by connecting both ends. The belt was wrapped around the pulleys ensuring the alignment direction of the azobenzene mesogens along the circular direction of the ring to guarantee a homogeneous movement direction. Similar laminated films were tested upon UV exposure at different intensities showing generation of mechanical force by photo-irradiation.

Afterward, Chen et al. (2010) developed a light-driven micropump by incorporating photo-isomerizable azobenzene moieties into the polyacrylate-based side-chain LC material. The reversible bending behavior of this material upon UV and visible light exposure is the responsible for inducing the membrane's movement and to pump a fluid. The working principle of the micropump, as well as a picture of the experimental prototype, is shown in Fig. 19.4c. Upon irradiation with UV light, the contraction gradient through the thickness of the film induces a downward bending which results in the reduction of the pump chamber volume, and the corresponding generation of pressure. In this way, the fluid in the chamber is forced to go to the pipe outlet. When the sample is exposed to visible light, a recovery of the film flatness is achieved by the upward bending of the film, and reduces the chamber's pressure which stops the flow.

Similar to the previously described microgripper (Sánchez-Ferrer et al. 2009), and following the actuation mechanism for the LCE-CNT composites (Li et al. 2012; Torras et al. 2014a), Petsch et al. (2014) introduced a novel approach based on the integration of deformable wires inside an active LC film. Then, a direct thermal actuation within the film is possible which results in a reduction of the actuation times—contraction and relaxation times—compared to other prior reported thermotropic polyacrylate-based side-chain LCE. Horseshoe platinum-gold-platinum micro-heaters were fabricated using standard MEMS/MOEMS technology processing on top of a polyimide (PI) layer and later, covered by a second PI layer to protect the conductive material and provide certain flexibility to the whole structure. Afterwards, all layers were structured using the reactive ion etching (RIE)

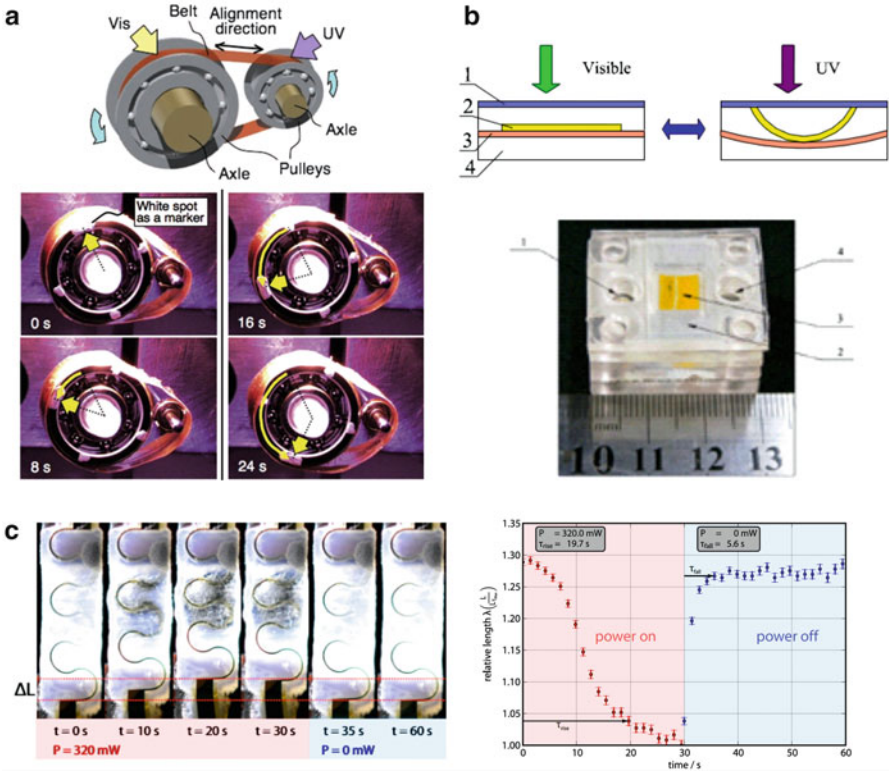

Fig. 19.4 Polyacrylate-based side-chain LCE actuators. (**a**) Alternated UV-visible photo-isomerization at different points of the azobenzene-containing LCE actuator ring which creates a local contraction and a local expansion of the belt and rotates the pulleys; (**b**) Micropump based on the bending motion of a LCE film which contains azobenzene moieties which upon UV-irradiation bends and with visible light relaxes back. (**c**) Sequence of thermo-resistors actuation showing changes in length and transparency of the LCE material upon heating and cooling under the application of 320 mW of electrical power

technique in order to obtain the heaters with their corresponding contact pads. A polyacrylate-based side-chain LC was synthesized following the process outlined by Thomsen et al. (2001) where all reagents were poured into a mold with the micro-heaters embedded by the reactive mixture. The material was aligned under a magnetic field, and finally photo-crosslinked by means of UV light. The contraction ratio of the actuator was measured as function of the electrical power applied. A contraction of 1.15 mm, which corresponds to relative change in sample's length of 1.28 was obtained at 320 mW, resulting in a 25.7 kPa of stress.

Basically, all actuation mechanisms described above are based on the conversion of an electrical current or electromagnetic fields into direct (microgripper, microvalve or embedded thermo-resistor actuator) or local heating (tactile device and heliotropic solar cell) which raises the temperature until reaching the isotropic

state. In principle, all mechanisms based on photo-isomerization of photoactive molecules (rotating belt and micropump) rely on the low temperature induced disorder when some molecules change their shape and acting as impurities. In principle, the latest mechanism should be a more efficient and faster process, but the process is slow at room temperature and depends on the irradiance, has some partial loss of the absorbed energy by non-radiative internal conversion or even emission, and the examples described here have a huge frictional factor and higher rigidity of the polymer backbone. All these factors lead towards actuation times of several minutes for the photoactive systems.

In this first section, various types of actuators has been described and their actuation mechanisms analyzed, all of them based on the integration of nematic side-chain LCE films which have been previously aligned and fully cross-linked. The main advantage of these actuators lies in that non-complex procedures are required for the integration. The nematic materials can be cut, fixed, or even glued, on different surfaces to form the final actuator. However, the main limitations of this type of actuators lie in their size, the shape and the type of orientation achieved by the LCE films—factors that are strongly related to the final response of the material, *i.e.*, deformation and movement direction. Similar to the MEMS/MOEMS fabrication processes, this free-standing oriented LCE films are perfect for the fabrication of actuators as a *Top-Down* approach, due to the possibility to pattern the oriented films in order to be adapted to the system for the manufacturing of devices.

19.3.2 Integration of In Situ *Fully-Crosslinked LCEs*

In contrast with the previously described systems based on the use of already aligned and fully crosslinked LCE films, in this section we analyze another concept for the fabrication of hybrid actuators consisting in the integration of partially crosslinked LCE films. Such films are then oriented and simultaneously cured in-situ. In this manner, it is possible to obtain LCE actuators in more complex shapes, far from the LCE films, with various types of alignment and not only limited to 1D. Thus, different types of actuation/deformation can be obtained leading to the fabrication of more elaborated actuators and devices.

This concept was firstly introduced by Buguin et al. (2006) which through replica molding combined with photo-crosslinking, and the application of magnetic fields, demonstrated the possibility to simultaneously shape, align and completely cure LCE material to create an array of thermoresponsive LCE pillars with contractions up to 40 %. Following this principle, different types of actuators have been reported so far, all of them based on molding techniques. Herein, we will describe all these actuators and the corresponding actuation principle analyzed. Similar to the previous section, they have been grouped as function of the type of chemistry used for their synthesis, as well as for their actuation mechanisms. The first three examples consist of elastomeric matrices based on polysiloxane chemistry, which

allows for lower range of actuation temperatures and relatively high deformations. The first one out of the three examples consists in a micropillar array with pushing properties based on direct heating. The other two examples, in both cases arrays of dome-like shaped actuators, are stood on photo-thermal actuation of LCE-CNTs nanocomposites. The last two actuators presented in this section consist in a micropillar array and an electrothermally driven photonic crystal, both based on photo actuation of polyacrylate-based LCE.

Torras et al. (2014b) followed the concept of replica molding outlined by of Buguin et al. (2006) to obtain micropillars with pushing properties using a polysiloxane matrix. In this manner, an array of nematic side-chain LCE actuators with elastic properties and low transition temperature was obtained, which produces direct actuation through heating, resulting in an expansion of the material. The pushing properties were reached by a two-step crosslinking process resulting in an array of micropushers. Such micropillars were oriented by uniaxial compression (biaxial orientation) instead of the classical uniaxial stretching procedure before the final curing. Thus, the micropillar array expands in the direction of the applied deformation when the isotropic temperature is reached ($T_{ni} \approx 55$ °C). This pushing behavior of the micropillars is related to the changes from the two-dimensional prolate polydomain conformation (nematic state) to the spherical conformation (isotropic state) of the polymer backbone. Figure 19.5 shows a scheme of the working principle of the proposed micropillars, as well as images of the fabrication process, and the main actuation results obtained. The resulting LCE micropillars with such novel orientation of the domains showed an expansion factor of $\varepsilon_z = 21$ % along the axial direction and a contraction factor of $\varepsilon_r = 15$ % in the radial direction upon isotropization, with an averaged dimensions of 3.63 mm in height and 2.10 mm in diameter in the isotropic phase, which resulted in actuation forces of about $F = 20$ mN (5.6 kPa of equivalent stress). These good results together with the possibility of obtaining different shapes on demand—besides the common LCE strip—make LCE materials very suitable candidates in the development of complex devices through their integration in Microsystems Technology and batch processes.

Camargo et al. (2011, 2012) demonstrated for the first time the possibility to obtain an array of actuating monodomains within the same polydomain matrix. Thanks to the use of an elaborated molding process similar to the punch and die stamping technique, together with a two-steps crosslinking process, sufficiently well-aligned LC units were created to produce localized actuation on a LCE-CNTs nanocomposite film upon illumination. Figure 19.6a schematically shows the stamping process and the working principle of the proposed actuators, where the aligned and non-aligned regions can be distinguished. A picture of the molding system and the actuators obtained, as well as a graph with the main actuation results, are also depicted. The fabrication process starts with a weakly-crosslinked film containing 0.1 wt% of MWCNTs which was placed in between two mold pieces, one containing pillars and the other one holes, and mechanically stretched to locally align the LC mesogens. Then, all the system was heated to thermally crosslink the film while keeping the mechanical load, resulting in an array of semi-spherical actuators of both 1.0 mm and 1.5 mm in diameter, with an alignment

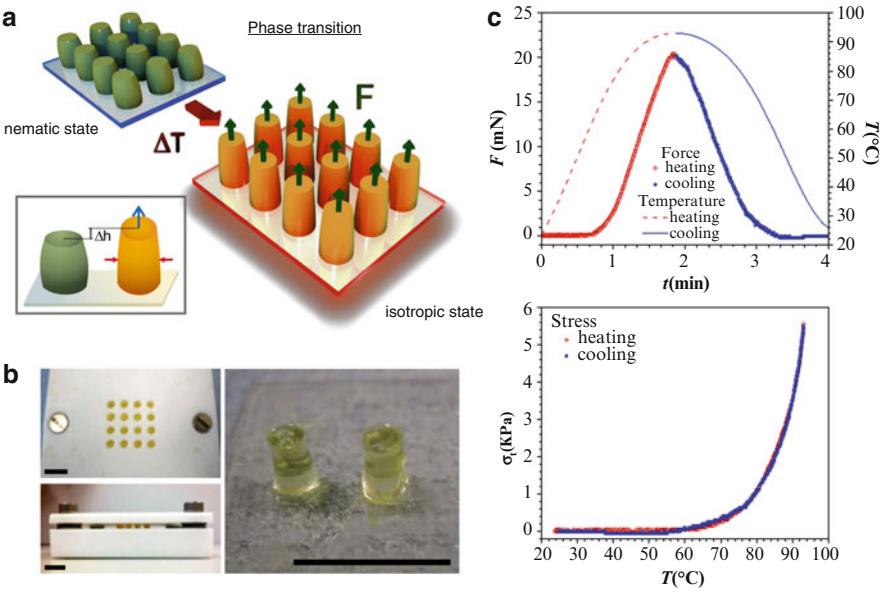

Fig. 19.5 (**a**) Scheme of the working principle of the proposed micropillars system resulting in pushing actuators under the application of thermal gradients. (**b**) Main steps for the micropillar fabrication where the molds, the orientation process through uniaxial compression, as well as an example of the actuators obtained previous the final crosslinking step can be observed (scale bars =10 mm). (**c**) Mechanical response of a single LCE micropillar along an entire heating-cooling cycle showing the pushing force as function of actuation temperature and time. 20 mN of force was obtained showing repeatability in response and no material degradation

normal to the direction of the film. For that reason, the dome-like shaped monodomain regions contract upon irradiation ($T_{ni} \approx 85$ °C) causing a decrease in their height, which reversibly return to their initial position when no light stimulus is applied. The response of the different actuators was analyzed using a red laser diode of 658 nm of wavelength as a light source at an incident optical power ranging from 8.6 mW to 51.5 mW, resulting up to 40 μm (10 %) of vertical displacement (contraction of $\varepsilon = 6.46$ %) in case of 1.5 mm of diameter actuators - deformation which is mainly limited by the dimensions of the punch mold. Moreover, on-off actuation cycles of the proposed actuators were performed to check the feasibility and repeatability in response, resulting in a low dispersion in contraction (less than 2.5 % of the mean value) without material degradation, leading to the use of this methodology for new applications in haptic devices.

Recently, Torras et al. (2014b) presented another interesting example using LCE-CNT nanocomposites. Inspired on the previous described method (Camargo et al. 2011, 2012), an alternative approach for the fabrication of arrays of semi-spherical actuators based on gas-pressure molding was proposed. It was demonstrated the possibility to shape and align LCE-CNT films by the application of a well-controlled nitrogen pressure. In this manner, a significant improvement on the

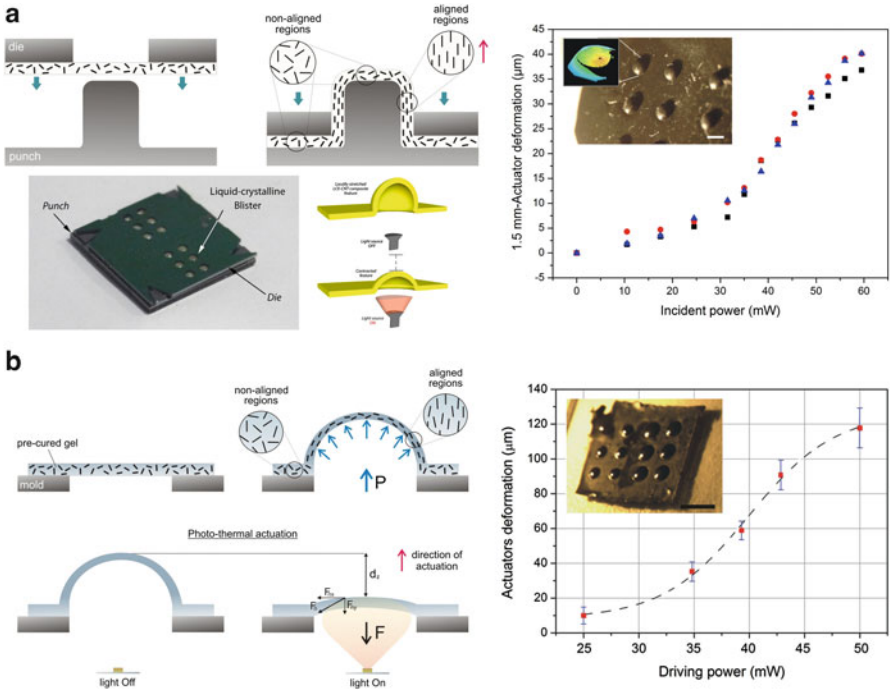

Fig. 19.6 Actuators arrays based on nematic LCE-CNT nanocomposites. Fabrication process and working principle of semi-spherical actuators array obtained by stamping molding (i.e., mechanical pressure) (**a**) and by the application of constant nitrogen flow (**b**). By using both approaches, aligned and non-aligned regions can be simultaneously produced, resulting in arrays of actuating features within a same LCE-CNT nanocomposite film. Under illumination, a reduction in height up to 40 μm and 120 μm were obtained respectively, as function of the optical power applied. Scale bars of pictures in the *insets* were 1 mm and 4 mm, respectively

deformation achieved by the actuators was obtained with respect to the reported by Camargo et al. (2011, 2012). The resulting height variation was up to 120 μm under illumination which mean contractions of $\varepsilon = 13$ % in the direction of the alignment under the application of 40 mbar of constant nitrogen pressure. A scheme showing the concept and the actuation principle of these actuators is presented in Fig. 19.6b, where also a graph with the main actuation results as function of the optical power applied are shown. Similar to the other system, this approach lies in the use of a two-steps crosslinking process which enables a correct shaping of the partially cross-linked material through molding process, and guarantees the application of the corresponding stress gradient to produce the desired deformation and alignment using nitrogen flow. Thus, arrays of identical dome-like shaped monodomain actuators can be obtained within the same polydomain LCE-CNT film with a perpendicular alignment, leading to local and reversible actuation. In this case,

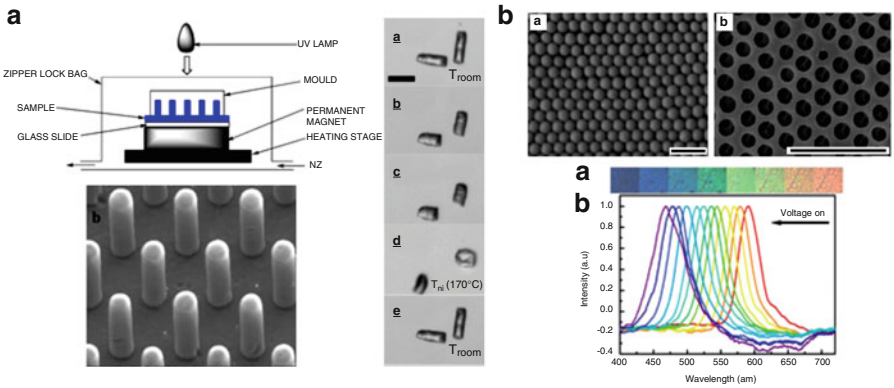

Fig. 19.7 Polyacrylate-based actuators in an array. (**a**) Schematic representation of the fabrication process of an array of thermoresponsive micropillars on a substrate by replica molding. Once the LCE pillars were completely cured they can be separated from the substrate and individually actuated by means of thermal gradients, resulting in high contraction movements ranging from 30 % to 40 %, as function of the acrylate matrix used (scale bar = 100 μm). (**b**) LCE Photonic crystal obtained by regular patterning of a LCE matrix through the embedding of a close-packed monodispersed silica particles' arrangement (scale bars = 1 μm)

LCE-CNT nanocomposites containing 0.3 wt% of MWCNTs were used, with transition temperatures of $T_g \approx 10$–15 °C and $T_{ni} = 90$ °C.

As previously mentioned at the beginning of this section, Buguin et al. (2006) introduced an innovative procedure for the fabrication of micron-sized thermoresponsive LCE actuators on a substrate by replica molding. In this manner, an array of nematic pillars of about 20 μm in diameter and 100 μm in height could be obtained in one single step. Firstly synthesized using side-on polyacrylate-based chemistry (Buguin et al. 2006) and then improved by using thiol-ene nematic main-chain LCE (Yang et al. 2009). The reported actuators show fully reversible contraction with values up to 30–40 % in the case of side-on LCE when heated from the nematic to the isotropic phases ($T_{ni} \approx 170$ °C). A scheme of the experimental setup for the fabrication of the micropillars together with a scanning electron microscopy (SEM) micrograph of the final structures and an actuation sequence are shown in Fig. 19.7a. A PDMS mold containing the patterns of the pillars which was prepared by replica molding was pressed down on the melted components of the nematic material forcing them to fill the inner structure of the mold, while a constant magnetic field of about 1 T was applied to ensure alignment of the nematic director parallel to the long axis of the pillars. Finally, the whole system was irradiated using a UV lamp to promote the LCE photo-polymerization. Each pillar can be removed from the array and used as a small actuator. However, such LCE materials are restricted to certain applications due to the elevated actuation temperatures (up to 170 °C), and thus they can neither be used in Biology for tissue engineering nor for cell culture studies.

Later on, Jiang et al. (2012) presented an innovative electrothermally driven photonic crystal based on the combination of nematic materials able to shift the

Bragg-diffraction peak under actuation, resulting on a structural change in color. Unlike the previous examples where a replica molding was used for the fabrication of non-continuous matrices of individual actuators (Torras et al. 2013; Buguin et al. 2006; Yang et al. 2009), Jiang et al. proposed an original method to pattern LCE matrices inspired by colloidal lithography processes in nanofabrication (Yang et al. 2006). They propose the use of a non-continuous 3D array of elements, in this case silica nanospheres (*i.e.*, an opaline photonic crystal), to create a continuous LCE films containing the inverse opaline structure, which acts as single photonic crystals. Figure 19.7b shows two SEM pictures of both types of structures, as well as a graph reflecting the photonic band-gap (PBG) shifts inducing structural color changes at 15 V of applied voltage and its corresponding normalized reflection spectra. For the preparation of the LCE photonic crystals, various layers of close-packed monodispersed nanosilica spheres were first prepared following the Stöber method (Stöber et al. 1968) and sandwiched between two glass plates, which were later immersed in the molten LCE solution to allow the mixture to completely fill the voids by capillary forces. Finally, the LC moieties were aligned and polymerized using UV-irradiation and the silica template etched by 1 wt% HF solution, resulting in the LCE-based inverse opaline structure. Spin-coated on a glass-substrate, graphite nanoparticles act as electrothermal conversion layer, delivering heat to the LCE structure and thus, forcing reversible changes on the optical response of the films, *e.g.*, displacement of the PBG and changes on the structural color of the films, as function of the electric voltage applied. Depending on the material composition, these inverse opaline structures show transition temperatures ranging from 20 °C to 32 °C and from 64 °C to 101 °C for the T_g and T_{ni}, respectively, as function of the crosslinking density.

In this second section various types of actuators have also been described and their actuation mechanisms analyzed, all of them based on the integration of nematic materials before the crosslinking process, allowing its in-situ alignment and curing in one single step. The main difficulties around these techniques lie in the various procedures involving the LCE material preparation, which require a very precise control of the whole device. Thus, the system should be conceived and fabricated taking into account the changes in dimensions and shape exhibited on the material during its alignment and crosslinking processes, which will strongly define the final type and degree of deformation achieved.

Unlike the methods described in the previous section, the main advantage of these techniques is that there is neither limitation in shape and size of the actuators obtained nor with the types of orientation defined. Thus, with an accurate design and the appropriate knowledge of the material, it is possible to fabricate a custom-made elaboration process to reach the desired response.

Seeking parallelism to conventional MEMS/MOEMS fabrication methods, one might consider this methodology to fabricate actuators such as *Bottom-up* approach, where the starting material at the molecular level is transformed and patterned at the same time for the obtaining of the macromolecular actuator already adapted to the system to form the device.

19.4 Conclusions and Outlook

LCEs are advanced, complex, and elaborated soft smart materials which require of expertise in Organic Synthesis, Macromolecular Chemistry and Physics, and Supramolecular Chemistry, as well as knowledge about Materials Science. The combination of the liquid state of order—from the liquid-crystalline molecules (mesogens)—and the rubber elasticity—from the polymer network (crosslinked polymer chains)—results on a material with unique mechanical and optical properties. The beauty of such materials stays in the control over the three components which allows for the obtaining of materials on demand. Thus, the precise selection of the mesogen nature leads towards different mesophases (*e.g.*, nematic, smectic, columnar, chiral, lyotropic phases), shifting of the isotropization temperature and the corresponding service temperature, and kind of coupling to the polymer backbone. While the choice on the polymer backbone brings flexibility (amorphous) or rigidity (glassy), variations in the crosslinking density contribute to the hardness (duromer) or softness (elastomer) of the final LCE material.

The main principle is the obtaining of monodomains of LCEs, where the mesogens are oriented and polymer chains aligned. Such anisotropic materials can undergo a spontaneous and reversible deformation accompanied by a retractive force when an external stimulus is applied and the liquid-crystalline order in the material is erased. The functionalization of such LCEs enables the material to interact with the environment. Thus, the incorporation of other molecules or functionalities increases the options for the use of other external stimuli besides temperature gradients, *e.g.*, light, magnetic or electric fields, electrical current, pH, ionic strength, solvent vapor. In this way, LCEs can convert any kind of energy into mechanical energy or vice versa.

The actuation principle for such LCEs markedly depends on the synthetic approach and the orientation/alignment technique used for the preparation of monodomains, as well as the external stimulus to be used. In principle, polycondensation-based LCEs (polysiloxane polymer backbone) are more suitable for contraction/expansion purposes, while polyaddition-based LCEs (poly(meth) acrylate polymer backbone) has mainly been used for bending modes. Nevertheless, both kinds of polymer backbones can develop any imaginable actuation movement, if a little bit of imagination and inventiveness is worked up.

When control over the actuation strain and stress, as well on the time response is accomplished, the next step is the integration of such LCEs into MEMS/MOEMS for the production of microdevices. Several examples have been described where the two possible approaches have been presented: the *ex situ* and *in situ* preparation of monodomains of LCEs. For the earlier, a *Top-Down* approach is followed for the integration of the material to the final device, while for the later a *Bottom-Up* approach is considered. The election for one or the other will be decided by the size, dimensions, shape and alignment of the LCE actuator together with the external stimulus to be used.

Due to the good integration of LCEs in Microsystems Technology, the applications offered by these hybrid MEMS/MOEMS range from the production of sensors to actuators for microrobotics, microoopotics and microfluidics. We are sure that in the near future new progresses in this area of miniaturization at the micro and nano scale will be seen when a better control on the mechanical and optical properties. For this purpose, and because of LCEs are the perfect material for such synergies, chemist, physicist and engineers should work together for the development of new devices. Still many open questions remain like the use of polydomains of LCEs, the energy efficiency improvement of such devices, the use of other mesophases, polymer architectures, functionalities and external stimuli.

References

Ajayan PM, Terrones M, de la Guardia A, Huc V, Grobert N, Wei BQ, Lezec H, Ramanath G, Ebbesen TW (2002) Nanotubes in a flash-ignition and reconstruction. Science 296:705

Berggren M, Nilsson D, Robinson ND (2007) Organic materials for printed electronics. Nature Mat 6:3

Beyer P, Terentjev EM, Zentel R (2007) Monodomain liquid crystal main chain elastomers by photocrosslinking. Macromol Rapid Commun 28:1485

Boussey J (2003) Microsystems technology: fabrication, test & reliability. Kogan Page, London

Brand HR, Finkelmann H (1998) Handbook of liquid crystals, vol 3. Wiley/VHC, Weinheim

Bründel M, Stubenrauch M, Wurmus H, Sánchez-Ferrer A (2004) Functional liquid-crystalline elastomers in Microsystems. Int Newslett Micro-Nano Integr (MSTNEWS) 4:38

Buguin A, Li MH, Silberzan P, Ladoux B, Keller P (2006) Micro-actuators: when artificial muscles made of nematic liquid crystal elastomers meet soft lithography. J Am Chem Soc 128:1088

Camargo CJ, Campanella H, Marshall JE, Torras N, Zinoviev K, Terentjev EM, Esteve J (2011) Localised actuation in composites containing carbon nanotubes and liquid crystalline elastomers. Macromol Rapid Commun 32:1953

Camargo CJ, Campanella H, Marshall JE, Torras N, Zinoviev K, Terentjev EM, Esteve J (2012) Batch fabrication of optical actuators using nanotube—elastomer composites towards refreshable Braille displays. J Micromech Microeng 22:075009

Cantournet S, Boyce MC, Tsou AH (2007) Micromechanics and macromechanics of carbon nanotube enhanced elastomers. J Mech Phys Solids 55:1321

Chambers M, Zalar B, Remškar M, Žumer S, Finkelmann H (2006) Actuation of liquid crystal elastomers reprocessed with carbon nanoparticles. Appl Phys Lett 89:243116

Chambers M, Finkelmann H, Remškar M, Sánchez-Ferrer A, Zalar B, Žumer S (2009) Liquid crystal elastomer—nanoparticle systems for actuation. J Mater Chem 19:1524

Chen M, Xing X, Liu Z, Zhu Y, Liu H, Yu Y, Cheng F (2010) Photodeformable polymer material: towards light-driven micropump applications. Appl Phys A 100:39

Cook-Chennault KA, Thambi N, Sastry AM (2008) Powering MEMS portable devices: a review of non-regenerative and regenerative power supply systems with special emphasis on piezoelectric energy harvesting systems. Smart Mater Struct 17:043001

Dai W, Lian K, Wang W (2007) Design and fabrication of a SU-8 based electrostatic microactuator. Microsyst Technol 13:271

Davis F (1993) Liquid-crystalline elastomers. J Mater Chem 3:551

de Gennes PG (1971) Nematic liquid crystals. J Phys Colloq 5:3

de Gennes PG (1975) Réflexions sur un type de polymères nématiques. C R Acad Sci Paris B 281:101

de Gennes PG (1993) The physics of liquid crystals, 2nd edn. Oxford University Press, New York
de Gennes PG (1997) A semifast artificial muscle. C R Acad Sci Series IIB 324:343
de Jeu WH (2012) Liquid crystal elastomers: materials and applications. Springer, Berlin
Dittrich PS, Manz A (2006) Lab-on-a-chip: microfluidics in drug discovery. Nat Rev Drug Discov 5:210
Donnio B, Wermter H, Finkelmann H (2000) A simple and versatile synthetic route for the preparation of main-chain, liquid-crystalline elastomers. Macromolecules 33:7724
Finkelmann H, Kock HJ, Rehage G (1981) Investigations on liquid crystalline polysiloxanes 3. Liquid crystalline elastomers: a new type of liquid crystalline material. Makromol Chem Rapid Commun 2:317
Finkelmann H, Kock HJ, Gleim W, Rehage G (1984) Investigations on liquid crystalline polysiloxanes, 5. Orientation of LC-elastomers by mechanical forces. Makromol Chem Rapid Commun 5:287
Finkelmann H, Nishikawa E, Pereira GG, Warner M (2001a) A new opto-mechanical effect in solids. Phys Rev Lett 87:015501
Finkelmann H, Greve A, Warner M (2001b) The elastic anisotropy of nematic elastomers. Eur Phys J E 5:281
Gad-el-Hak M (2005) MEMS: applications. CRC, Boca Raton
Grayson ACR, Shawgo RS, Johnson AM, Flynn NT, Li YW, Cima MJ, Larger R (2004) A BioMEMS review: MEMS technology for physiologically integrated devices. Procc IEEE 92:6
Haberl JM, Sánchez-Ferrer A, Mihut AM, Dietsch H, Hirt A, Mezzenga R (2013) Liquid-crystalline elastomer-nanoparticle hybrids with reversible switch of magnetic memory. Adv Mater 25:1787
Haberl JM, Sánchez-Ferrer A, Mihut AM, Dietsch H, Hirt AM, Mezzenga R (2014) Light-controlled actuation, transduction, and modulation of magnetic strength in polymer nanocomposites. Adv Funct Mater 24:3179
Haeberle S, Zengerle R (2007) Microfluidic platforms for lab-on-a-chip applications. Lab Chip 7:1094
Hardouin F, Leroux N, Noirez N, Keller P, Mauzac M, Achard MF (1994) Small angle neutron scattering (SANS) studies on "side-on fixed" liquid crystal polymers. Mol Cryst Liq Cryst 254:267
Haseloh S, Zentel R (2009) Synthesis of liquid-crystalline colloids in nonpolar media and their manipulation in electric fields. Macromol Chem Phys 210:1394
Hogan PM, Tajbakhsh AR, Terentjev EM (2002) UV manipulation of order and macroscopic shape in nematic elastomers. Phys Rev E 65:041720
Hsu TR (2008) MEMS & microsystems: design, manufacture, and nanoscale engineering, 2nd edn. Wiley, Hoboken
Huber J, Fleck NA, Ashby MF (1997) The selection of mechanical actuators based on performance indices. Proc R Soc Lond A 453:2185
Ji Y, Huang YY, Rungsawang R, Terentjev EM (2010) Dispersion and alignment of carbon nanotubes in liquid crystalline polymers and elastomers. Adv Mater 22:3436
Ji Y, Huang YY, Terentjev EM (2011) Dissolving and aligning carbon nanotubes in thermotropic liquid crystals. Langmuir 2:13254
Ji Y, Marshall JE, Terentjev EM (2012) Nanoparticle-liquid crystalline elastomer composites. Polymers 4:316
Jiang Y, Xu D, Xuesong L, Lin C, Li W, An Q, Tao C, Tang H, Li G (2012) Electrothermally driven structural colour based on liquid crystal elastomers. J Mater Chem 22:11943
Jiang H, Li C, Huang X (2013) Actuators based on liquid crystalline elastomer materials. Nanoscale 5:5225
Judy JW (2001) Microelectromechanical systems (MEMS): fabrication, design and application. Smart Mater Struct 10:1115
Kaiser A, Winkler M, Krause S, Finkelmann H, Schmidt AM (2009) Magnetoactive liquid crystal elastomer nanocomposites. J Mater Chem 19:538

Knežević M, Warner M (2013) Optomechanical elastomeric engine. Phys Rev E 062503:1
Komp A, Rühe J, Finkelmann H (2005) A versatile preparation route for thin free-standing liquid single crystal elastomers. Macromol Rapid Commun 26:813
Krause S, Dersch R, Wendorff JH, Finkelmann H (2007) Photocrosslinkable liquid crystal main-chain polymers: thin films and electrospinning. Macromol Rapid Commun 28:2062
Kremer F, Skupin H, Lehmann W, Hartmann L, Stein P, Finkelmann H (2000) Structure, mobility, and piezoelectricity in ferroelectric liquid crystalline elastomers. Adv Chem Phys 113:183
Kundler I, Finkelmann H (1998) Director reorientation via stripe-domains in nematic elastomers: influence of cross-link density, anisotropy of the network and smectic clusters. Macromol Chem Phys 199:677
Küpfer J, Finkelmann H (1991) Nematic liquid single crystal elastomers. Macromol Chem Rapid Commun 12:717
Küpfer J, Finkelmann H (1994) Liquid crystal elastomers: influence of the orientational distribution of the crosslinks on the phase behaviour and reorientation processes. Macromol Chem Phys 195:1353
Lehmann O (1908) Biologisches Centralblatt 28:31
Lehmann WL, Hartmann L, Kremer F, Stein P, Finkelmann H, Kruth H, Diele S (1999) The inverse electromechanical effect in mechanically oriented Sc*-elastomers examined by means of an ultra-stable Michelson interferrometer. J Appl Phys 86:1647
Leondes CT (2006) MEMS/NEMS: handbook. Springer, New York
Li MH, Keller P, Li B, Wang X, Brunet M (2003) Light-driven side-on nematic elastomer actuators. Adv Mater 15:569
Li C, Liu Y, Lo C, Jiang H (2011) Reversible white-light actuation of carbon nanotube incorporated liquid crystalline elastomer nanocomposites. Soft Matter 7:7511
Li C, Liu Y, Huang X, Jiang H (2012) Direct sun-driven artificial heliotropism for solar energy harvesting based on a photo-thermomechanical liquid-crystal elastomer nanocomposite. Adv Funct Mater 22:5166
Liu C (2007) Recent developments in polymer MEMS. Adv Mater 19:3783
Lorenz H, Despont M, Fahrni N, LaBianca N, Renaud P, Vettiger P (1997) SU-8: a low-cost negative resist for MEMS. J Micromech Microeng 7:121
Lutz G (1999) Semiconductor radiation detectors. Springer, Berlin
Maluf N, Williams K (2003) An introduction to microelectromechanical systems engineering, 2nd edn. Artech House, Boston
Marshall JE, Ji Y, Torras N, Zinoviev K, Terentjev EM (2012) Carbon-nanotube sensitized nematic elastomer composites for IR-visible photoactuation. Soft Mater 8:1570
Merlos A, Acero M, Bao MH, Bausells J, Esteve J (1993) TMAH/IPA anisotropic etching characteristics. Sensor Actuat A-Phys 37:737
Noirez L, Keller P, Davidson P, Hardouin F, Cotton JP (1988) Backbone conformation study of a side chain polyacrylate through a re-entrant polymorphism. J Phys France 49:1993
Ohm C, Serra C, Zentel R (2009) A continuous flow synthesis of micrometer-sized actuators from liquid crystalline elastomers. Adv Mater 21:4859
Ohm C, Brehmer M, Zentel R (2010) Liquid crystalline elastomers as actuators and sensors. Adv Mater 22:3366
Petsch S, Rix R, Reith P, Khatri B, Schuhladen S, Ruh D, Zentel R, Zappe H (2014) A thermotropic liquid crystal elastomer micro-actuator with integrated deformable micro-heater. Proc MEMS 905
Plaza JA, Collado A, Cabruja E, Esteve J (2002) Piezoresistive accelerometers for MCM package. J Micromech Syst 11:794
Saito R, Dresselhaus G, Dresselhaus MS (1998) Physical properties of carbon nanotubes, vol 4. Imperial College Press, London
Sánchez-Ferrer A (2011) Light-induced disorder in liquid-crystalline elastomers for actuation. Proc SPIE 8107:810702

Sánchez-Ferrer A, Finkelmann H (2009) Mechanical deformations in smectic-c main-chain liquid-crystalline elastomers. Mol Cryst Liq Cryst 508:348
Sánchez-Ferrer A, Finkelmann H (2013) Opto-mechanical effect in photoactive nematic main-chain liquid-crystalline elastomers. Soft Matter 9:4621
Sánchez-Ferrer A, Fischl T, Stubenrauch M, Wurmus H, Hoffmann M, Finkelmann H (2009) Photo-crosslinked side-chain liquid-crystalline elastomer for microsystems. Macromol Chem Phys 210:1671
Sánchez-Ferrer A, Merekalov A, Finkelmann H (2011a) Opto-mechanical effect in photoactive nematic side-chain liquid-crystalline elastomers. Macromol Rapid Commun 32:672
Sánchez-Ferrer A, Fischl T, Stubenrauch M, Albrecht A, Wurmus H, Hoffmann M, Finkelmann H (2011b) Liquid-crystalline elastomer microvalve for microfluidics. Adv Mater 23:4526
Schätzle J, Finkelmann H (1987) Lyotropic liquid crystalline phase behavior of amphiphilic monomers and polymers having a rod-like hydrophobic moiety. Mol Cryst Liq Cryst 142:85
Snyder GJ, Lim JR, Huang CK, Fleurial JP (2003) Thermoelectric microdevice fabricated by a MEMS-like electrochemical process. Nature Mater 2:528
Stöber W, Fink A, Bohn E (1968) Controlled growth of monodisperse silica spheres in the micron size range. J Colloid Interface Sci 26:62
Tajbakhsh AR, Terentjev EM (2001) Spontaneous thermal expansion of nematic elastomers. Eur Phys J E 6:181
Terentjev EM (1999) Liquid-crystalline elastomers. J Phys Condens Matter 11:R239
Thomsen DL, Keller P, Naciri J, Pink R, Jeon H, Shenoy D, Ratna BR (2001) Liquid crystal elastomers with mechanical properties of a muscle. Macromolecules 34:5868
Tombler TW, Zhou C, Alexseyev L, Kong J, Dai H, Liu L, Jayanthi CS, Tang M, Wu SY (2000) Reversible electromechanical characteristics of carbon nanotubes under local-probe manipulation. Nature 405:769
Torras N, Zinoviev KE, Esteve J, Sánchez-Ferrer A (2013) Liquid-crystalline elastomer micropillar array for haptic actuation. J Mater Chem C 1:5183
Torras N, Zinoviev KE, Camargo CJ, Campo EM, Campanella H, Esteve J, Marshall JE, Terentjev EM, Omastová M, Krupa I, Teplicky P, Mamojka B, Bruns P, Roeder B, Vallribera M, Malet R, Zuffanelli S, Soler V, Roig J, Walker N, Wenn D, Vossen F, Crompvoets FMH (2014a) Tactile device based on opto-mechanical actuation of liquid crystal elastomers. Sensor Actuat A-Phys 208:104
Torras N, Marshall JE, Zinoviev KE, Camargo CJ, Terentjev EM, Esteve J (2014b) Gas-pressure molding-based fabrication of smart actuators from nematic liquid-crystalline elastomer. Macromol Mater Eng 299:1163
Urayama K (2010) Stimulus-responsive nematic gels. Macromol Symp 291–292:89
Urayama K, Honda S, Takigawa T (2006) Deformation coupled to director rotation in swollen nematic elastomers under electric fields. Macromolecules 39:1943
Urayama K, Mashita R, Kobayashi I, Toshikazu T (2007) Stretching-induced director rotation in thin films of liquid crystal elastomers with homeotropic alignment. Macromolecules 40:7665
Wang XJ, Warner M (1987) Theory of nematic comb-like polymers. J Phys A 20:713
Warner M, Terentjev EM (2007) Liquid crystal elastomers. Clarendon, Oxford
Wermter H, Finkelmann H (2001) Liquid crystalline elastomers as artificial muscles. e-Polymers 013:1–13
Winkler M, Kaiser A, Krause S, Finkelmann H, Schmidt AM (2010) Liquid crystal elastomers with magnetic actuation. Macromol Symp 291–292:186
Woltman S, Jay G, Crawford G (2007) Liquid-crystal materials find a new order in biomedical applications. Nature Mat 6:929
Xia YN, Whitesides GM (1998) Soft lithography. Annu Rev Mater Sci 28:153
Yamada M, Kondo M, Mamiya J, Yu Y, Kinoshita M, Barret CJ, Ikeda T (2008) Photomobile polymer materials: towards light-driven plastic motors. Angew Chem Int Ed 47:4986
Yang R, Wang W (2004) Out-of-plane polymer refractive microlens fabricated based on direct lithography of SU-8. Sensor Actuat A Phys 113:71

Yang SM, Jang SG, Choi DG, Kim S, Yu HK (2006) Nanomachining by colloidal lithography. Small 2:458

Yang H, Buguin A, Taulemesse JM, Kaneko K, Méry S, Bergeret A, Keller P (2009) Micron-sized main-chain liquid crystalline elastomer actuators with ultralarge amplitude contractions. J Am Chem Soc 131:15000